remote sensing

MDPI

Article

Canopy Fluorescence Sensing for In-Season Maize Nitrogen Status Diagnosis

Rui Dong [1], Yuxin Miao [2,*], Xinbing Wang [3], Fei Yuan [4] and Krzysztof Kusnierek [5]

[1] College of Resources and Environmental Sciences, China Agricultural University, Beijing 100193, China; BS20183030296@cau.edu.cn
[2] Precision Agriculture Center, Department of Soil, Water and Climate, University of Minnesota, St. Paul, MN 55108, USA
[3] Institute of Crop Sciences, Chinese Academy of Agricultural Sciences, Beijing 100081, China; wangxinbing@caas.cn
[4] Department of Geography, Minnesota State University, Mankato, MN 56001, USA; fei.yuan@mnsu.edu
[5] Center for Precision Agriculture, Norwegian Institute of Bioeconomy Research (NIBIO), Nylinna 226, 2849 Kapp, Norway; krzysztof.kusnierek@nibio.no
* Correspondence: ymiao@umn.edu

Abstract: Accurate assessment of crop nitrogen (N) status and understanding the N demand are considered essential in precision N management. Chlorophyll fluorescence is unsusceptible to confounding signals from underlying bare soil and is closely related to plant photosynthetic activity. Therefore, fluorescence sensing is considered a promising technology for monitoring crop N status, even at an early growth stage. The objectives of this study were to evaluate the potential of using Multiplex® 3, a proximal canopy fluorescence sensor, to detect N status variability and to quantitatively estimate N status indicators at four key growth stages of maize. The sensor measurements were performed at different growth stages, and three different regression methods were compared to estimate plant N concentration (PNC), plant N uptake (PNU), and N nutrition index (NNI). The results indicated that the induced differences in maize plant N status were detectable as early as the V6 growth stage. The first method based on simple regression (SR) and the Multiplex sensor indices normalized by growing degree days (GDD) or N sufficiency index (NSI) achieved acceptable estimation accuracy (R^2 = 0.73–0.87), showing a good potential of canopy fluorescence sensing for N status estimation. The second method using multiple linear regression (MLR), fluorescence indices and GDDs had the lowest modeling accuracy (R^2 = 0.46–0.79). The third tested method used a non-linear regression approach in the form of random forest regression (RFR) based on multiple sensor indices and GDDs. This approach achieved the best estimation accuracy (R^2 = 0.84–0.93) and the most accurate diagnostic result.

Keywords: fluorescence sensing; nitrogen status; multiple linear regression; machine learning; precision nitrogen management

Citation: Dong, R.; Miao, Y.; Wang, X.; Yuan, F.; Kusnierek, K. Canopy Fluorescence Sensing for In-Season Maize Nitrogen Status Diagnosis. *Remote Sens.* **2021**, *13*, 5141. https://doi.org/10.3390/rs13245141

Academic Editors: Bruno Basso and Ignacio A. Ciampitti

Received: 10 November 2021
Accepted: 15 December 2021
Published: 17 December 2021

1. Introduction

Nitrogen (N) is one of the most important macronutrients for crop growth that strongly influences crop photosynthesis and gross primary productivity [1,2]. Inappropriate N fertilization can reduce crop yield due to N deficiency or lead to negative environmental impacts due to N surplus [3–5]. Therefore, it is imperative and necessary to assess the N status effectively and understand crop N demand to guide producers to make proper N management decisions.

The methods for determining crop N status have been intensely studied and thoroughly discussed. The traditional laboratory wet-chemical methods to determine N concentration in crops are based on destructive sampling and are labor-intensive and time-consuming. To overcome these shortcomings and realize high efficiency in modern agriculture, sensing technology has shown great potential in assessing crop N status

and providing site-specific diagnosis via real-time and non-invasive detection. Canopy reflectance sensing has been commonly used for estimating crop N status and guiding in-season N management. Active canopy sensors with their own light sources are not limited by ambient lighting conditions and are very suitable for practical on-farm applications [6–9]. They have been used to estimate the N status of diverse crops, including wheat (*Triticum aestivum* L.), rice (*Oryza sativa* L.), and maize (*Zea mays* L.), and as valuable tools for site-specific N management [10–13]. However, reflectance signals are affected by soil background, and it is challenging to estimate chlorophyll or N concentration as canopy reflectance is also influenced by leaf area index and biomass [14]. Early detection of crop N stress is very important for crop growers to make management decisions. However, reflectance-based indices can only indicate the macroscopic variations in crops, such as a decrease in biomass accumulation rate and yellowing of leaves, which are results of long-term N stress in the plants. They cannot effectively detect physiological traits that have already occurred in plants before visible symptoms appear [15,16]. It is known that plant N concentration (PNC) is strongly related to plant chlorophyll concentration, which is important for photosynthetic activity. There is a fluorescence emission phenomenon in chlorophyll molecules in plant leaves. Thus, crop N status could also be evaluated using fluorescence signals. As an innovation in assessing crop N status, fluorescence sensors have the advantages of less influence from soil background and the high correlation with chlorophyll and N concentration [14,16–18]. In addition, being related to plant photosynthetic activity, fluorescence spectroscopy has been considered a potentially emerging technology for early monitoring of crop N status that would be observed before the obvious changes in the amount of chlorophyll in the leaves [19,20].

In recent years, there has been increasing interest in the application of fluorescence sensing in agriculture to improve N management. Two commercial devices are most commonly used: Dualex (FORCE-A, Orsay, Paris, France) and Multiplex (FORCE-A, Orsay, Paris, France). Compared with Dualex that features three fluorescence-based indices and measures on a small area of leaf scale, Multiplex is a more efficient canopy sensor and offers several fluorescence parameters. However, studies focused on the applications of Multiplex sensors are rather scarce, especially for the evaluation of the N status of maize. Although previous studies have revealed the relationships between Multiplex parameters and applied N rates and determined the possibility of using Multiplex to detect N variability in maize, they only focused on the early growth stages in greenhouses [17,21]. However, understanding and assessing N across different growth stages under field conditions is crucial for in-season site-specific N management applications.

Choosing appropriate N status indicators is critical for crop N monitoring. Since the measurements are solely based on the changes of pigments in leaves, fluorescence sensing is less susceptible to erroneous signals from bare soil; hence, it is more related to N concentration than reflectance-based parameters, especially at early growth stages before canopy closure or in wide-row crops [14,16,20]. Thus, many researchers have explored and verified the ability of Multiplex to estimate PNC [22–24], plant N uptake (PNU), and N nutrition index (NNI) [18,25], and explored the feasibility for in-season N recommendation [26–29].

Previous studies have indicated that low N diagnostic accuracy was achieved using the NNI estimated by a direct method based on a single spectral index [30,31]. Due to the influence of factors other than N, such as the time factor (i.e., growth stage), it might be challenging to estimate N indicators by remote sensing [8,32,33]. Many methods have been developed to reduce the impact of these factors and improve estimation accuracy. Some spectral parameters were modified to establish better relationships with N indicators using simple regression (SR) models. Among them, the application of the normalized N sufficient index (NSI) is a very common procedure that has been used in many studies [18,32,34]. A recent study proposed a modified approach to estimate maize PNC across growth stages based on the use of days after sowing (DAS) [35].

In addition, other remote sensing algorithms for crop N retrieval, using empirical, physical, and hybrid methods based on multiple parameters have been widely adopted in

recent years. Multiple linear regression (MLR) is suitable for processing linear relationships of complex data, and it is often used due to its simplicity and acceptable performance. Non-linear regression methods are becoming increasingly popular in crop N monitoring due to their reliable and robust performance, particularly when handling large amounts of data [36–38]. Random forest regression (RFR) is one of the most widely used machine-learning methods, which can overcome the overfitting and collinearity problems that are prone to occur in linear approaches, and often yields higher estimation accuracies [8,39–41].

As maize is a major staple grain crop and requires large amounts of N fertilizer, it is particularly important to assess variations of maize N status and implement precision N management practices. Fluorescence sensing has proven to be a promising technology for monitoring crop growth, but studies on applications of Multiplex sensors for maize under field conditions are limited. There is a lack of reports exploring promising methods to efficiently estimate maize N status across growth stages. Thus, the objectives of this study were to: (1) assess the usability of the fluorescence parameters of Multiplex sensor for detection of N variability under different N rate treatments at different growth stages; and (2) evaluate and compare different methods (SR, MLR, and RFR models) to estimate N status indicators (PNC, PNU and NNI) across different growing conditions.

2. Materials and Methods

2.1. Experimental Design

The field experiments were carried out in Lishu County (43°02′–43°46′ N, 123°45′–124°53′ E), Jilin Province in Northeast China from 2017 through 2019. Detailed information about daily mean temperature (°C) and rainfall (mm) during the growing season of the experimental years is shown in Figure 1. The soil type at the study site is classified as Typic Haploboroll according to the United States Department of Agriculture (USDA)'s soil taxonomy. A randomized complete block design with split plots including planting density as the main plots and N rate as the subplots was set up in the experiments, with each plot size being 9 m × 12 m = 108 m^2. Spring maize cultivar Liangyu 66 was planted at densities of 5.5, 7.0, and 8.5 plants m^{-2}. Six N rates (0, 60, 120, 180, 240, 300 kg ha^{-1}) were included with 1/3 of the total fertilizer applied before sowing as basal N using ammonium sulfate and 2/3 applied at around V8-V9 stage as side-dress N using urea. Each treatment was replicated three times. Sufficient phosphorus (90 kg ha^{-1} P_2O_5) and potassium (90 kg ha^{-1} K_2O) fertilizers were applied before sowing together with N fertilizers. A wide-narrow row planting pattern was adopted with sowing spacing of 80−40 cm. The field was kept free of weeds, insects, and diseases with pesticides based on local standard practices. Irrigation measures were conducted after sowing for the lack of rainfall in 2018 and 2019 to ensure seedling emergence.

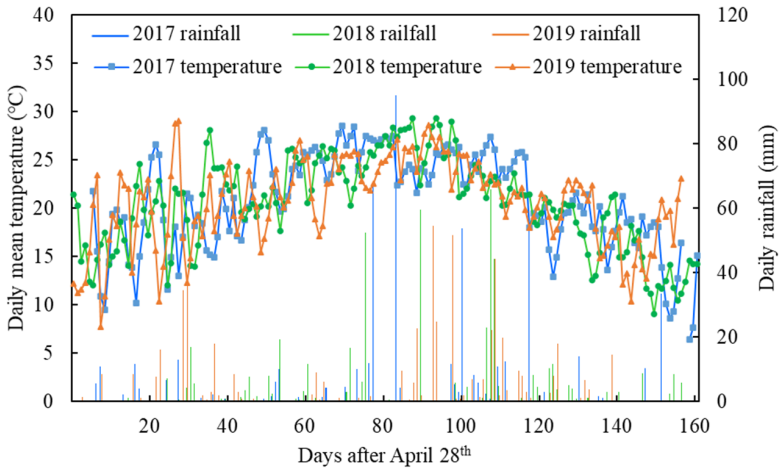

Figure 1. Daily mean temperature (°C) and rainfall (mm) during the growing season in the experimental years.

2.2. Fluorescence Sensing

At the V4, V6, V8, and VT growth stages [42] in 2017, the V3 and V5 growth stages in 2018, and the V6, V8, V12, and VT growth stages in 2019, proximal sensing measurements were made using a fluorescence sensor Multiplex® 3 (FORCE-A, Orsay, France). Multiplex is an ultraviolet (UV)-visible portable fluorimeter involving four excitation channels (UV, blue, green, and red) to generate fluorescence in the plant tissues and three synchronized filtered detectors to record the fluorescence in yellow (590 nm, YF), red (665 nm, RF) and far-red (735 nm, FRF) bands. In addition to the eleven fluorescence indices provided by the sensor, six additional indices were calculated in this study, considering their good performance in previous research [18,21,22,25]. These indices included simple chlorophyll fluorescence ratio (SFR) related to leaf chlorophyll content, calculated under green (SFR_G) or red (SFR_R) illumination, FLAV for indicating flavonols content and ANTH for indicating anthocyanin content, and N balance index (NBI) taking into account both the content of chlorophyll and flavonols, calculated under green (NBI_G) or red (NBI_R) illumination. A detailed overview of the fluorescence parameters used is given in Table 1.

Table 1. Description of the parameters provided by Multiplex used in this study.

Multiplex Parameter	Description	Excitation	Formula
YF_UV	UV excited yellow fluorescence	UV	–
RF_UV	UV excited red fluorescence	UV	–
FRF_UV	UV excited far-red fluorescence	UV	–
YF_B	Blue excited yellow fluorescence	Blue	–
RF_B	Blue excited red fluorescence	Blue	–
FRF_B	Blue excited far-red fluorescence	Blue	–
YF_G	Green excited yellow fluorescence	Green	–
RF_G	Green excited red fluorescence	Green	–
FRF_G	Green excited far-red fluorescence	Green	–
RF_R	Red excited red fluorescence	Red	–
FRF_R	Red excited far-red fluorescence	Red	–
SFR_G	Green excited simple fluorescence ratio	Green	FRF_G/RF_G
SFR_R	Red excited simple fluorescence ratio	Red	FRF_R/RF_R
FLAV	Red and UV excited flavonols	Red and UV	Log (FRF_R/FRF_UV)
ANTH	Red and green excited anthocyanins	Red and Green	Log (FRF_R/FRF_G)
NBI_G	UV and green excited nitrogen balance index	UV and Green	FRF_UV/RF_G
NBI_R	UV and red excited nitrogen balance index	UV and Red	FRF_UV/RF_R

The Multiplex sensor was placed above the maize canopy before the V8 growth stage with a measurement mask of the sensor just touching the canopy, and on leaf scale around the most recently fully expanded leaves at the V12 growth stage and around ear leaves at the VT growth stage. The measurements were made manually at approximately 10 cm above the adaxial (top) side of the leaf, on a circular surface of 50 cm^2 with a diameter of 8 cm. The measurements were not taken at a fixed time on each sensing date since the sensor is not influenced by ambient light conditions [16]. The fluorescence data were collected from plants located in the inner rows of each plot, and the average value was used to represent the plot.

2.3. Sampling and Measurement

At the V6, V8, and VT growth stages in 2017, and at the V6, V8, V12, and VT growth stages in 2019, three representative plants located in the rows of each plot measured by the Multiplex sensor were sampled at the ground level. All samples were separated into leaves and stems except for the V6 growth stage. All leaves and stems of the three plant samples from each plot were mixed together for N analysis. After being dried at 105 °C for half an hour, the samples were then dried at 70 °C until they maintained a constant weight.

The N concentrations of leaves and stems of each plot were determined using the modified Kjeldahl method [43]. The PNC was calculated using the following formula:

$$PNC = (W_l \times N_l + W_s \times N_s)/(W_l + W_s) \quad (1)$$

where W_l and W_s stand for the weights of the leaves and stems, respectively, and N_l and N_s stand for the N concentrations of leaves and stems, respectively.

The PNU is the product of PNC and aboveground biomass (t ha^{-1}), while the NNI is defined as the ratio of the actual PNC to the critical N concentration (N_c), which was calculated according to a critical N dilution curve for spring maize [44]:

$$N_c = 36.5\ W^{-0.48} \quad (2)$$

where W is the aboveground biomass (t ha^{-1}). The value of N_c was set up to a constant value of 36.5 for plants with aboveground biomass lower than 1 t ha^{-1}, because the critical N dilution curve cannot be applied to these plants [44].

2.4. Regression Models to Estimate N Status Indicators

The SR, MLR, and RFR methods were employed to establish general models to estimate N status indicators across growth stages and years and compared in this study. Six Multiplex indices were involved in these models, including SFR_G, SFR_R, FLAV, ANTH, NBI_G, and NBI_R. When using SR models, these six Multiplex indices were also modified by combing with growing degree days (GDD, °C) for PNC and PNU estimation and converted into NSI (SFR_G_{SI}, SFR_R_{SI}, $FLAV_{SI}$, $ANTH_{SI}$, NBI_G_{SI}, and NBI_R_{SI}), which equals to the ratio of the sensor reading of a plot to the well-fertilized (300 kg N ha^{-1}) plot for NNI estimation, besides the raw readings. Linear, quadratic, power, exponential, and logarithmic functions were adopted to simulate the relationships between sensing indices and N status indicators to select the best performing functional equation for validation.

The GDD was calculated from the date of seedling emergence to the date of sensing measurements at each growth stage using the following formula:

$$GDD = \Sigma\ ((T_{max} - T_{min})/2 - T_{base}) \quad (3)$$

where T_{max}, T_{min}, T_{base} are the daily maximum, minimum, and base temperatures, respectively. T_{base} was set to 10 °C. Detailed information on GDD of the four key growth stages used for N status estimation is shown in Table 2.

Table 2. Growing degree days (GDD, °C) of different growth stages in 2017 and 2019.

Experimental Year	V6	V8	V12	VT
2017	229.8	392.7	–	880.0
2019	271.1	406.8	605.1	808.1

Both the MLR and RFR models were developed based on the GDD information, and all the six Multiplex indices were used as the input data. The scikit-learn, a Python machine learning library [45], was used in this study to conduct the RFR analysis. A repeated sampling method, 10-fold cross-verification, and grid search were adopted to adjust the RFR model and find the optimal parameters.

2.5. Statistical Analysis

A total of 54 data points at each growth stage in each year was acquired. All the Multiplex signals and indices obtained at the respective growth stages under six N rate treatments were used to assess the performance of N variability detection. The fluorescence data were subjected to analysis of variance (ANOVA), and a Duncan test was used to compare the means for each treatment at the $p < 0.05$ significance level. Reference data obtained from sampled plants and six Multiplex indicators (SFR_G, SFR_R, FLAV, ANTH,

NBI_G, and NBI_R) collected from the V6 to VT growth stages in 2017 and 2019 were used to estimate N status indicators (PNC, PNU, and NNI) using SR, MLR and RFR models (Figure 2). About 67% (36 data points at each growth stage in each year) of the data collected from all plots were used to train the regression models, and the remaining data (18 data points at each growth stage in each year) were used to test the models as validation dataset. The coefficient of determination (R^2), the root mean square error (RMSE), and relative error (RE) were used as validation metrics. In addition, the kernel density curves of the observed and estimated values of N indicators were plotted using OriginPro 2019b (OriginLab Corporation, Northampton, MA, USA) to further compare the accuracies. Kernel density estimation is a popular tool for estimating the probability density function of a random variable and visualizing the distribution of data in a non-parametric way [46]. To evaluate the diagnostic accuracy of different regression models, NNI values were divided into three classes, and the value within the range of < 0.95, 0.95 to 1.05, and > 1.05 indicates N deficit, optimal, and surplus, respectively [47]. The areal agreement and Kappa statistics were calculated [48,49]. A higher Kappa value indicates a higher diagnostic accuracy. The Kappa values of 0.01–0.20, 0.21–0.40, 0.41–0.60, 0.61–0.80, and 0.81–0.99 represent slight, fair, moderate, substantial, and almost perfect agreement, respectively [48].

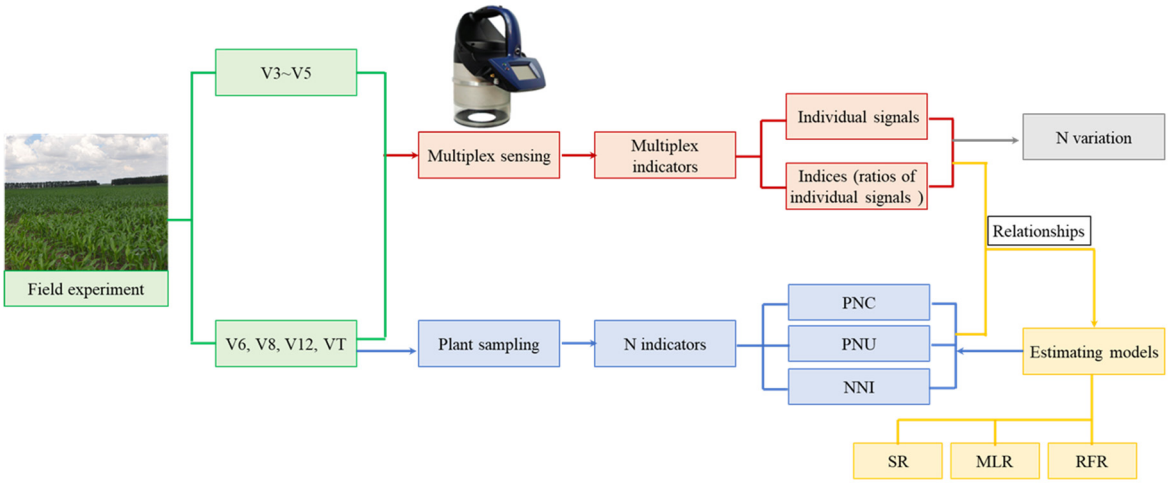

Figure 2. Flow chart of the methodology to use Multiplex sensing parameters for maize N variability detection and N indicators estimation. PNC, PNU and NNI stand for plant N concentration, plant N uptake and N nutrient index, respectively. SR, MLR and FRF stand for simple regression, multiple linear regression and random forest regression, respectively.

3. Results

3.1. Differences in Fluorescence Parameters at Different N Rates

According to the ANOVA results of Multiplex parameters, as affected by the six N rates at each growth stage, the effect of N fertilization treatment on most of the individual signals was not significant whereas the opposite was true for the fluorescence indices calculated from the individual signals (Table 3). The SFR_G, SFR_R, NBI_G, and NBI_R increased with the increase of applied N, while decreasing trends were found for FLAV and ANTH (Figure 3). Although the N treatment affected some fluorescence indices based on the ratio of individual signals before the V6 stage (SFR_G and SFR_R obtained at the V3 and V4 stages, FLAV obtained at the V5 stage, NBI_G and NBI_R obtained from the V3 to V5 stages) (Table 3), in most cases these indices could only distinguish between N and non-N treatments (Figure 3). For all indices (fluorescence ratios), except for ANTH, the preferred distinction among the N treatments was observed starting from the V6 growth stage (Table 3 and Figure 3). However, all the tested fluorescence indices were not sensitive to N rates ranging from 180 to 300 kg ha^{-1} N at the V6 growth stage, and most of them failed to distinguish the two high N rates (240 and 300 kg ha^{-1}) during the V8 to VT growth phase. Comparatively, NBI_G and NBI_R showed the best discrimination ability and could

detect differences between 240 and 300 kg ha^{-1} at some of the later growth stages, followed by SFR_G and SFR_R. The two polyphenol-related indices (ANTH and FLAV) performed not as well as the abovementioned indices, especially for ANTH, which performed the worst in all growth stages (Figure 3).

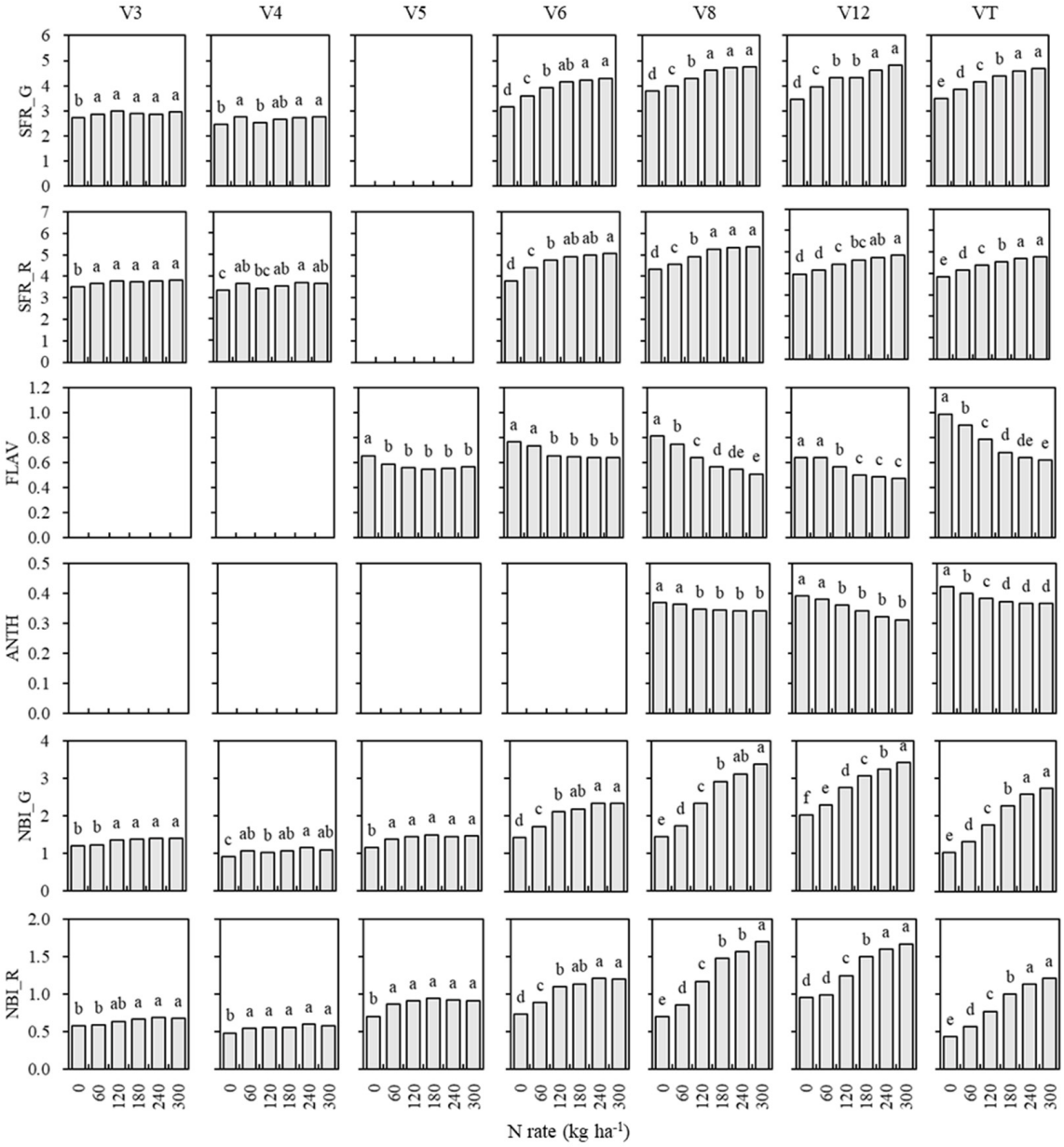

Figure 3. Average values of Multiplex indices as affected by N rates at different growth stages. Different letters indicate significant differences according to the Duncan test at $p < 0.05$ significance level. $n = 54$ for V3, V4, V5 and V12, and $n = 108$ for V6, V8 and VT.

Table 3. Analysis of variance (ANOVA) of Multiplex parameters at different growth stages as affected by six N rates for maize.

Multiplex Parameter	V3 (n = 54)	V4 (n = 54)	V5 (n = 54)	V6 (n = 108)	V8 (n = 108)	V12 (n = 54)	VT (n = 108)
YF_UV	ns	ns	ns	ns	ns	ns	ns
RF_UV	ns	*	ns	***	***	***	***
FRF_UV	*	*	ns	***	***	***	***
YF_B	ns	ns	ns	ns	ns	***	ns
RF_B	ns	ns	ns	ns	ns	ns	ns
FRF_B	ns	ns	ns	ns	ns	ns	ns
YF_G	ns	ns	ns	ns	ns	***	**
RF_G	ns	ns	ns	ns	ns	ns	ns
FRF_G	*	ns	ns	***	ns	*	ns
RF_R	ns	ns	ns	ns	ns	ns	ns
FRF_R	*	ns	ns	**	ns	ns	ns
SFR_G	**	**	ns	***	***	***	***
SFR_R	**	**	ns	***	***	***	***
FLAV	ns	ns	***	***	***	***	***
ANTH	ns	ns	ns	ns	***	***	***
NBI_G	**	***	***	***	***	***	***
NBI_R	**	**	***	***	***	***	***

***: Significant at $p < 0.001$ level; **: Significant at $p < 0.01$ level; *: Significant at $p < 0.05$ level; ns: not significant at $p < 0.05$ level.

3.2. Simple Regression Analysis for Relationships between Raw Multiplex Indices and N Status Indicators

The relationships between the Multiplex indices and maize N status indicators for an individual year and across years at different growth stages were studied by fitting experimental data with linear functions. The R^2 values and significance levels are shown in Table 4. Almost all of the relationships were significant at the $p < 0.001$ level, nonetheless, the lowest R^2 values appeared at the V6 growth stage. Most fluorescence indices acquired at the V6 and V8 growth stages from the canopy level were more related to N status indicators within a specific year than across the years. However, the situation at the VT growth stage was different, with similarly high R^2 values at each individual year and across the years. Overall, most of the best-fitted linear functions were based on NBIs.

To estimate maize N status across growth stages and experimental years, SR relationships between fluorescence indices and the three N indicators were developed using the best-fitted model types (Table 5). Among them, the fluorescence indices were more related to NNI when gathering all data under different treatments together. However, all these functions had low R^2 values ranging from 0.07 to 0.40 (Table 5).

Table 4. The coefficients of determination (R^2) for the linear relationships between Multiplex indices and N status indicators at each growth stage.

N Indicator	Year	SFR_G	SFR_R	FLAV	ANTH	NBI_G	NBI_R	SFR_G	SFR_R	FLAV	ANTH	NBI_G	NBI_R
					V6						**V8**		
PNC ($g\ kg^{-1}$)	2017	0.31 ***	0.38 ***	0.28 ***	0.14 *	0.62 ***	0.61 ***	0.72 ***	0.73 ***	0.73 ***	0.46 ***	0.78 ***	0.78 ***
	2019	0.48 ***	0.53 ***	0.36 ***	0.15 *	0.58 ***	0.61 ***	0.69 ***	0.73 ***	0.69 ***	0.26 **	0.71 ***	0.74 ***
	Across years	0.34 ***	0.36 ***	0.25 ***	0.05 *	0.57 ***	0.60 ***	0.30 ***	0.61 ***	0.32 ***	0.06 *	0.28 ***	0.38 ***
PNU ($kg\ ha^{-1}$)	2017	0.43 ***	0.41 ***	0.24 **	0.22 **	0.48 ***	0.40 ***	0.59 ***	0.64 ***	0.78 ***	0.49 ***	0.80 ***	0.81 ***
	2019	0.46 ***	0.55 ***	0.21 ***	0.12 ***	0.44 ***	0.47 ***	0.70 ***	0.75 ***	0.70 ***	0.41 ***	0.69 ***	0.73 ***
	Across years	0.12 **	0.13 **	0.31 ***	0.38 ***	0.21 ***	0.39 ***	0.62 ***	0.64 ***	0.64 ***	0.41 ***	0.67 ***	0.73 ***
NNI	2017	0.31 ***	0.38 ***	0.28 ***	0.14 *	0.62 ***	0.61 ***	0.67 ***	0.71 ***	0.80 ***	0.49 ***	0.84 ***	0.85 ***
	2019	0.48 ***	0.53 ***	0.36 ***	0.15 *	0.58 ***	0.61 ***	0.73 ***	0.78 ***	0.72 ***	0.37 ***	0.73 ***	0.77 ***
	Across years	0.34 ***	0.36 ***	0.25 ***	0.05 *	0.57 ***	0.60 ***	0.56 ***	0.73 ***	0.60 ***	0.28 ***	0.59 ***	0.68 ***
					V12						**VT**		
PNC ($g\ kg^{-1}$)	2017	–	–	–	–	–	–	0.57 ***	0.53 ***	0.71 ***	0.67 ***	0.70 ***	0.72 ***
	2019	0.62 ***	0.68 ***	0.56 ***	0.49 ***	0.76 ***	0.76 ***	0.75 ***	0.69 ***	0.58 ***	0.54 ***	0.80 ***	0.82 ***
	Across years	–	–	–	–	–	–	0.66 ***	0.61 ***	0.63 ***	0.45 ***	0.74 ***	0.75 ***
PNU ($kg\ ha^{-1}$)	2017	–	–	–	–	–	–	0.65 ***	0.59 ***	0.80 ***	0.68 ***	0.82 ***	0.82 ***
	2019	0.73 ***	0.61 ***	0.64 ***	0.60 ***	0.83 ***	0.78 ***	0.81 ***	0.69 ***	0.60 ***	0.68 ***	0.81 ***	0.83 ***
	Across years	–	–	–	–	–	–	0.73 ***	0.65 ***	0.68 ***	0.53 ***	0.80 ***	0.80 ***
NNI	2017	–	–	–	–	–	–	0.66 ***	0.61 ***	0.80 ***	0.71 ***	0.81 ***	0.82 ***
	2019	0.75 ***	0.67 ***	0.65 ***	0.61***	0.86 ***	0.82 ***	0.82 ***	0.70 ***	0.61 ***	0.68 ***	0.83 ***	0.84 ***
	Across years	–	–	–	–	–	–	0.74 ***	0.66 ***	0.69 ***	0.53 ***	0.80 ***	0.81 ***

***: Significant at $p < 0.001$ level; **: Significant at $p < 0.01$ level; *: Significant at $p < 0.05$ level; –: No data.

Table 5. The best-fitted model types and R^2 values of SR relationships between N indicators and raw Multiplex indices across growth stages and experimental years.

Raw Multiplex Index	PNC (g kg^{-1})		PNU (kg ha^{-1})		NNI	
	Model	R^2	Model	R^2	Model	R^2
SFR_G	Q	ns	P	0.31 ***	Q	0.31 ***
SFR_R	Q	0.24 ***	Q	0.12 ***	Q	0.26 ***
FLAV	E	0.14 ***	P	0.12 ***	Q	0.30 ***
ANTH	E	0.09 ***	E	0.07 ***	Q	0.14 ***
NBI_G	P	0.10 ***	E	0.20 ***	Q	0.38 ***
NBI_R	P	0.21 ***	E	0.12 ***	Q	0.40 ***

***: Significant at $p < 0.001$ level; ns: Not significant at $p < 0.05$ level; Q, E and P stand for quadratic, exponential and power models, respectively.

3.3. General Models for Estimating N status Indicators

3.3.1. Simple Regression Models Based on Normalized Multiplex Indices

Multiplex indices were modified to develop models that can be used across growth stages and years. To estimate PNC and PNU that generally vary significantly with growth stages, GDD that introduce the information about the age of the plants was used together with Multiplex indices. As NNI is a ratio and relatively stable across growth stages and years, the NSI values of each raw Multiplex index were calculated to estimate NNI. The R^2 values of the SR models based on the normalized indices fitted with quadratic or power functions were significantly enhanced compared with the models based on raw indices, although the degree of change was different (Tables 5 and 6). The greatest improvement was found in the relationships with PNC, with the highest increased R^2 values (from 0.09–0.24 to 0.73–0.85). In contrast, small changes to R^2 were found in the NNI results (from 0.14–0.40 to 0.38–0.68). Modified NBIs were the indices most related to PNU and NNI, while the modified SFRs and the two polyphenol indicators showed the best correlations with PNC.

Table 6. Best-performing fitted model types and R^2 values of simple regression models between N indicators and normalized Multiplex indices across years and growth stages.

PNC (g kg^{-1})			PNU (kg ha^{-1})			NNI		
Modified Multiplex Index	Model	R^2	Modified Multiplex Index	Model	R^2	Modified Multiplex Index	Model	R^2
SFR_G/GDD	Q	0.83 ***	SFR_G×GDD	Q	0.70 ***	SFR_G_{SI}	Q	0.46 ***
SFR_R/GDD	Q	0.85 ***	SFR_R×GDD	Q	0.66 ***	SFR_R_{SI}	Q	0.46 ***
FLAV×GDD	P	0.83 ***	FLAV/GDD	P	0.79 ***	$FLAV_{SI}$	Q	0.61 ***
ANTH×GDD	P	0.84 ***	ANTH/GDD	P	0.63 ***	$ANTH_{SI}$	P	0.38 ***
NBI_G/GDD	Q	0.73 ***	NBI_G×GDD	Q	0.84 ***	NBI_G_{SI}	Q	0.65 ***
NBI_R/GDD	Q	0.79 ***	NBI_R×GDD	Q	0.81 ***	NBI_R_{SI}	Q	0.68 ***

***: Significant at $p < 0.001$ level; Q and P stand for quadratic and power models, respectively.

3.3.2. Multiple Linear Regression and Random Forest Regression Models

The six Multiplex indices for each growth stage were combined to estimate the three N status indicators using the MLR and RFR methods with the addition of the corresponding GDD information. Although the MLR models were based on many fluorescence indices, they did not explain more variabilities of the three N indicators than the SR models built on the modified Multiplex indices (Tables 6 and 7). The most promising general models for estimating N status indicators across years and growth stages were simulated using the non-linear RFR method, which showed the highest R^2 values (0.96–0.99) (Table 7).

Table 7. R^2 values and coefficients of variables in multiple linear regression (MLR) models and relative importance (Gini coefficients) of estimated variables in random forest regression (RFR) models for estimating N status indicators across years and growth stages.

N Status Indicator	GDD	SFR_G	SFR_R	FLAV	ANTH	NBI_G	NBI_R	Constant	R^2
				MLR					
PNC (g kg^{-1})	−0.0300	7.498	−0.334	−21.448	106.555	−19.254	31.548	−9.085	0.76 ***
PNU (kg ha^{-1})	0.127	23.646	−4.027	−90.184	−109.662	−6.879	8.226	8.243	0.77 ***
NNI	0.0000137	0.311	−0.0670	−0.811	2.045	−0.432	0.831	−0.320	0.41 ***
				RFR					
PNC (g kg^{-1})	0.770	0.0087	0.135	0.0106	0.00686	0.0322	0.0374	–	0.99 ***
PNU (kg ha^{-1})	0.471	0.318	0.061	0.028	0.016	0.024	0.082	–	0.97 ***
NNI	0.255	0.164	0.107	0.021	0.015	0.158	0.281	–	0.96 ***

***: Significant at $p < 0.001$ level.

The detailed information of the MLR and RFR models is presented in Table 7. In the MLR models, the GDD had a smaller impact on N status indicators with obviously lower coefficients compared with fluorescence variables. In contrast, a large fraction of the variation explained using the RFR model was due to the addition of GDD. In particular, GDD ranked first in the estimations of PNC and PNU and ranked second in the estimation of NNI (Table 7).

3.3.3. Validation of the Regression Models

The performance of the SR models based on the modified Multiplex indices, MLR, and RFR models was validated using an independent dataset. In general, the SR models outperformed the MLR models for the estimations of all N status indicators (Table 8 and Figure 4a–f). The lower R^2 (0.46 to 0.79), larger RMSE (0.19 to 17.77), and RE (24.04% to 38.85%) along with larger dispersion of the sample points in the scatter plots indicated that the combination of multiple fluorescence indices and GDD incorporated in the MLR method did not perform well in estimating the three maize N status indicators across years and growth stages. Additionally, the most evident difference in the density curves between the estimated and observed N status indicators further confirmed the poor performance of MLR models (Figure 5). The MLR model for NNI estimation produced the lowest areal agreement, with no significant Kappa values (Table 9).

The RFR method demonstrated the absolute superiority to retrieve maize N status quantitatively when incorporating Multiplex indices and GDD into the algorithm (Figure 4). Although the improvement in R^2, RMSE, and RE for PNU estimation using the RFR model was not significant compared with using the SR model based on the best-performing modified index (NBI_G×GDD), the better-distributed points in the scatter plot and the resultant closer linear fitting line to 1:1 line implied higher accuracy. The RFR method generated the most similar distribution of the estimated N indicators to that of the observed N indicators as shown by the kernel density curves (Figure 5). What's more, according to the N status diagnosis results using NNI calculated with modified NBI_R and RFR model in Table 9, both methods achieved high areal agreements (0.72 and 0.77 respectively) and Kappa values over 0.40. The RFR model performed the best, with the highest accuracy in the diagnosis of N nutrition status.

Table 8. Validation results of the simple regression models based on the modified Multiplex indices for estimating N status indicators across years and growth stages.

PNC (g kg^{-1})				PNU (kg ha^{-1})				NNI			
Modified Multiplex Index	R^2	**RMSE**	**RE**	**Modified Multiplex Index**	R^2	**RMSE**	**RE**	**Modified Multiplex Index**	R^2	**RMSE**	**RE**
SFR_G/GDD	0.82 ***	4.31	20.89%	SFR_G×GDD	0.71 ***	20.95	45.79%	SFR_G_{SI}	0.59 ***	0.17	20.88%
SFR_R/GDD	0.84 ***	4.11	19.88%	SFR_R×GDD	0.64 ***	23.09	50.48%	SFR_R_{SI}	0.56 ***	0.17	21.74%
FLAV×GDD	0.87 ***	3.68	17.84%	FLAV/GDD	0.79 ***	17.52	38.30%	$FLAV_{SI}$	0.68 ***	0.15	18.60%
ANTH×GDD	0.83 ***	4.20	20.36%	ANTH/GDD	0.62 ***	23.80	52.03%	$ANTH_{SI}$	0.37 ***	0.21	25.88%
NBI_G/GDD	0.76 ***	4.99	24.18%	NBI_G×GDD	0.86 ***	14.21	31.06%	NBI_G_{SI}	0.71 ***	0.14	17.64%
NBI_R/GDD	0.82 ***	4.29	20.77%	NBI_R×GDD	0.85 ***	15.16	33.15%	NBI_R_{SI}	0.73 ***	0.14	17.03%

***: Significant at $p < 0.001$ level.

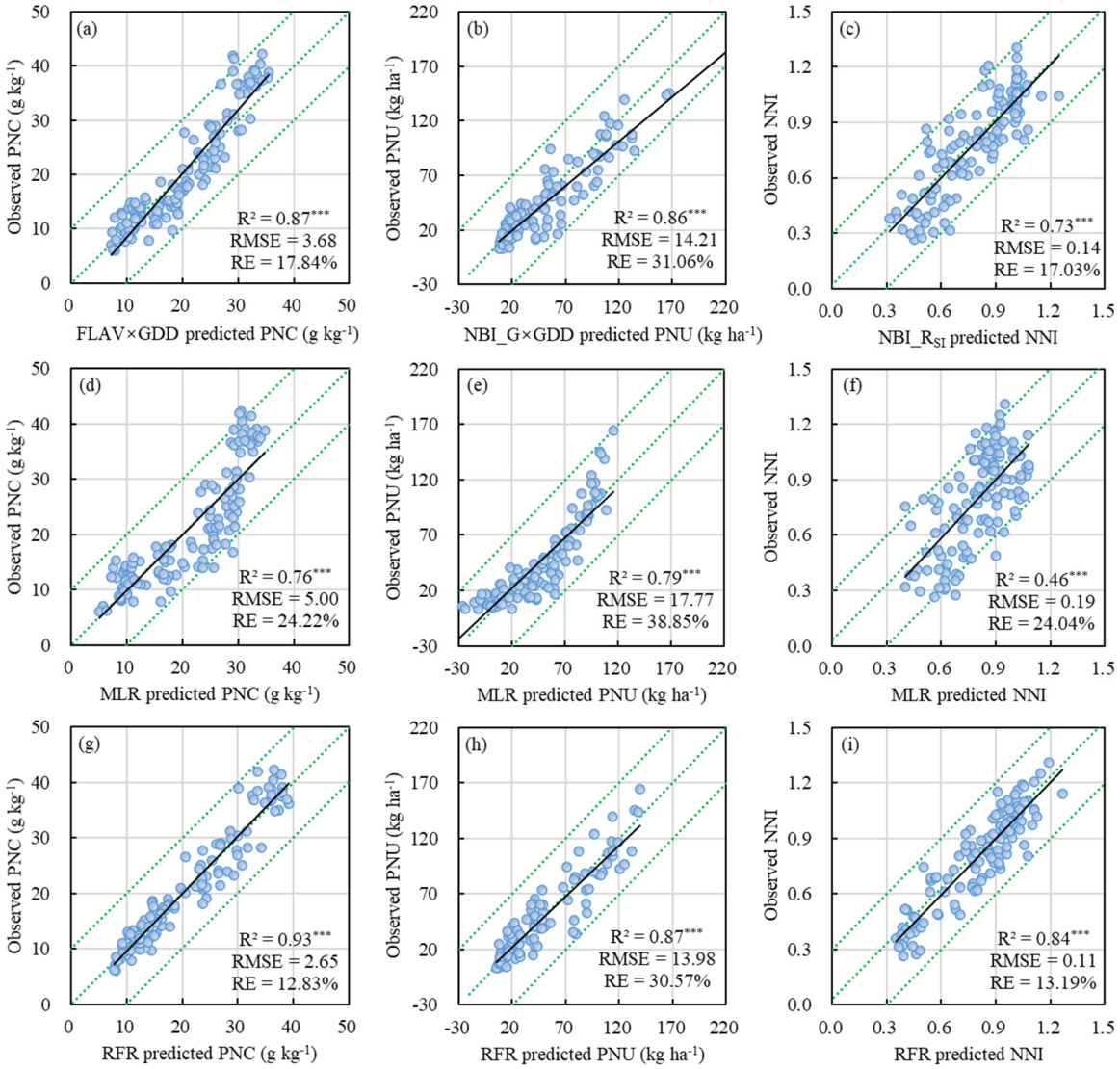

Figure 4. Validation results for estimating N status indicators across years and growth stages using simple regression (SR) models based on the best performed normalized Multiplex indices (**a**–**c**), multiple linear regression (MLR) models (**d**–**f**) and random forest regression (RFR) models (**g**–**i**). ***: Significant at $p < 0.001$ level.

Table 9. Areal agreement and Kappa statistics of the diagnostic results based on the estimated NNI derived from the best-performing modified Multiplex index (NBI_R_{SI}), multiple linear regression (MLR) model and random forest regression (RFR) model across years and growth stages.

	NBI_R_{SI}	MLR	RFR
Areal agreement	0.72	0.59	0.77
Kappa statistics	0.45 ***	0.06 ^{ns}	0.55 ***

***: Significant at $p < 0.001$ level; ^{ns}: Not significant at $p < 0.05$ level.

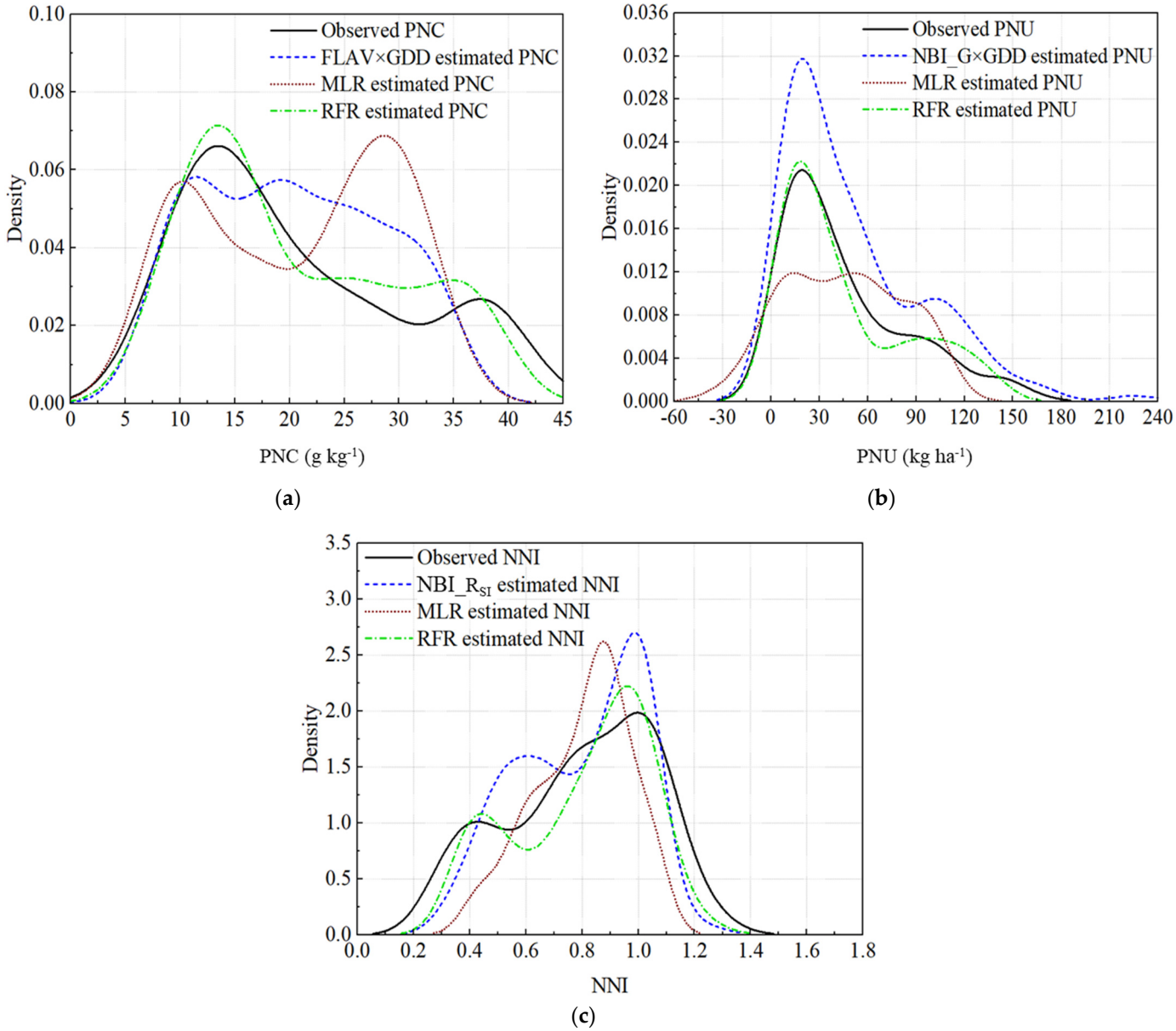

Figure 5. Kernel density plots of observed and predicted N indicators using simple regression (SR) models based on the best-performing modified Multiplex indicators, multiple linear regression (MLR) models and random forest regression (RFR) models across years and growth stages: (**a**) plant N concentration (PNC); (**b**) plant N uptake (PNU); (**c**) N nutrition index (NNI).

4. Discussion

4.1. Detection of N Variability in Maize Using Fluorescence Parameters

To determine if active canopy fluorescence sensing can detect N rate differences in maize plants at early growth period for making N management decisions, the sensing measurements were conducted before the V8 growth stage and as early as the V3 growth stage. Besides, the V12 and VT growth stages were also included in this study, because some remedial management actions could be taken. Most of the individual fluorescence signals in this study failed to distinguish the difference among different N supplies, whether in the early or later period of the maize growth process (Table 3). This is inconsistent with the reported results of maize from V2 to V6 stages in an earlier publication [21]. However, the additional straw treatment (straw was incorporated into the soil before sowing) without N fertilizer in their research might have played a major role in causing significant differences

in maize N status. This could be reflected by the significantly higher mean values of another Multiplex index calculated from an individual signal, fluorescence excitation ratio anthocyanin relative index (FERARI, Log (5000/FRF_R)) under the treatment of straw incorporation. Nevertheless, Tremblay et al. pointed out that the fluorescence ratios as a result of the combinations of independent signals were potentially useful to interpret crop N status [16]. This statement has been supported by many studies [17,23,25,50], and the results of this study confirmed the above-mentioned conclusion that the combined Multiplex indices based on the ratios of individual fluorescence signals could estimate maize N status effectively (Table 3 and Figure 3).

Although most Multiplex indices were significantly affected by N treatment from the V3 to V5 growth stages, they only enabled the distinction of low N rates (especially for 0 kg ha^{-1} N rate) in this study area (Table 3 and Figure 3). This is because maize plants do not require extensive N in the early growing period. The limited plant N demand can be met by a low N supply, which would delay the measurable reduction of pigments related to N [32]. What's more, because of the important interference within the measuring height range of 20 cm from the ground [17], the occurrence of weeds may also affect the Multiplex sensing of some crops with low plant height at the seeding stage.

The perfect distinction among the N treatments using the Multiplex indices was observed from the V6 growth stage (Figure 3). However, they all failed to differentiate N treatments ranging from 180 to 300 kg ha^{-1} at this starting period (V6). From this stage, maize plants began to absorb more nutrients. This outcome could probably be attributed to the fact that plants located in the plots with relatively abundant basal N supply had not yet fully responded to N shortages, especially in newly expanded leaves monitored by the sensor at the canopy level due to N transfer from lower leaves to upper-level leaves. This period is slightly different from the one identified by Longchamps and Khosla, who reported the perfect performance of NBI excited by green and red wavelengths, beginning from the V7 growth stage based on pot tests conducted in a greenhouse [17]. Different experimental conditions may have resulted in this delayed response. Maize plants grown in the field would suffer from more environmental stresses which may trigger an additional fluorescence emission. In most cases, the Multiplex indices could not discriminate N rates between 240 and 300 kg ha^{-1} during the growing season (Figure 3). Similar insensitivity of Multiplex sensor to high N rates also occurred in other studies [22,25]. Simulated by a crop model (CERES-Maize) based on field experiments and historical weather information, the long-term economic optimal N rate in this study site was found to be 198 $\pm$ 35 kg ha^{-1} [51]. However, after reaching the optimal N level, little excessive N was accumulated by luxury N uptake, and the N concentration in maize plants did not change significantly [35]. This led to the indistinctive variation of the fluorescence indices under the two high N rates.

FLAV and ANTH changed inversely with the N rate due to polyphenols accumulation in leaf epidermis under lower N availability, which was opposite to the increasing trend of SFRs related to chlorophyll content [52,53]. Overall, the two indices displayed weaker N differentiation ability (especially ANTH). The sensitivity of polyphenols to plant physiological states, such as the occurrence of senescence, and other stresses caused by low temperature and light intensity may be a reasonable explanation [54–56]. Influenced by both chlorophylls and flavonoids, NBI is independent of leaf mass per area and has a wide response range as a result of the inverse changes of SFR and FLAV, which makes it a more robust and reliable indicator of N status [22,34].

4.2. Development of General Models to Estimate Maize N Status Indicators

The six Multiplex indices were further used to evaluate maize N status quantitatively from the V6 to VT growth stages in view of their preferred detection of N variability during this period. Maize plant starts to absorb greater amounts of N from the V6 growth stage at the beginning of rapid stem elongation. Sufficient N supply before the V8 growth stage is essential to guarantee yield [57]. Therefore, at the V6 to V8 growth stages, it is early enough to estimate N status indicators to make N recommendations. Moreover, assessment of

N during the rest of the vegetative growth phase would provide a valuable indication of expected yield and grain quality. Thus, continuous monitoring of crop N during all growth phases could be of important meaning [58]. Two later growth stages were also included in maize N status evaluation in this study.

4.2.1. Limitations for Developing General Models

Successful establishment of reliable relationships between sensor readings and plant N status indicators, especially across site-years and growth stages, may be affected by various factors such as experimental and environmental variables [32,33]. Multiplex indices were less related to N status indicators with lower R^2 values at the V6 growth stage, compared with other growth stages. This might have resulted from the relatively poor capacity in N variation differentiation of these fluorescence indices within the range of 180 to 300 kg ha^{-1} at this growth period discussed above. Most of the direct linear relationships within each year were quite good and significant at the $p < 0.001$ level (Table 4), indicating the applicability and potential of the tested fluorometric sensor for estimating N-related crop indicators in a single environment.

Inconsistent variations in most of the Multiplex indices and N status indicators resulted in evidently lower R^2 values at the V6 and V8 growth stages. Changes in these variables were small at the VT growth stage, leading to similarly high R^2 values for individual years and across years. When using data collected from all growth stages across the two years, the results of the SR models based on single raw Multiplex indices were unsatisfactory. The major challenges of developing crop stress detection algorithms throughout the season and across spaces have been summarized by Pinter et al. [59]. Recently, Berger et al. also pointed out the necessity to take the time factor into account [8]. As environmental conditions (such as temperature) change over time, they might be the key determinants of fluorescence emission by influencing pigment contents in leaves [60,61].

The superiority of NBI as a reliable and robust indicator for crop N status assessment has been demonstrated in previous studies [18,22,23,25]. In this study, the high sensitivity for detecting N variations and the high R^2 in the SR linear relationships related to NBIs also strongly supported this conclusion. It has been suggested that a single fluorescence index may not always be enough to yield good N status estimates over the entire crop growth period in different years, while combining indices and spectral mixing analysis is a potential way to overcome this limitation [62,63]. Considering the similar or better performance of some other fluorescence indices in several cases (Table 4, Table 6, and Table 8), data fusion methods may perform better and should be further explored.

4.2.2. Comparison of Different Regression Models

To reduce the influence of different years and growth stages on the general model, GDD was adopted to identify temporal changes in our study. With the advantages of simple structure and few input parameters, the SR method was prioritized in this study, due to its popularity and ease of use. As revealed by previous studies [35,47], PNC showed a significant decreasing trend while PNU showed a significant increasing trend as maize growth. However, the values of Multiplex indices were relatively stable at different growth stages. The GDD is a good indicator of crop growth and development during the growing period. In addition, the crops may display changed physiological status and influence the relationships between crop N status and sensing parameters in different years even at the same growth phase [64,65], partly due to weather conditions [32]. The combination of GDD using multiplication or division method could help to increase the variation of Multiplex indicators at different growth stages just like the PNC and PNU, and help to identify the seasonal variation at the same time. Therefore, satisfactory results were observed when estimating PNC and PNU using the SR models (Tables 6 and 8). The GDD information may not be needed for seasonally stable N indicators, such as NNI, which had good correlations with Multiplex indices across years and growth stages (Tables 4 and 5). Another normalization method, the calculation of NSI, was suggested to be useful for

reducing the influence of external factors and maintaining the stability of sensing indices throughout the season and across years [18,66,67]. The NSI normalization was therefore employed in the establishment of SR models for NNI estimation. In general, significant improvements of estimation power were achieved for all three N status indicators using the SR models by modifying the sensing indices. Nevertheless, some PNU values were apparently overfitted (Figure 4b), and the accuracy of the validation results was not satisfactory as the density curves of the estimated values differed greatly from those of the observed values (Figure 5).

Hence, the MLR and RFR methods based on data fusion were further explored for N assessment. For the developed MLR models, GDD showed a minor role in the functions with significantly lower coefficients among all variables (Table 7). In addition, although multiple variables were combined, the MLR models performed the worst and had the least accurate estimation of N status indicators, and failed to diagnose N status (Table 9). In this study, fluorescence indices accounted for most of the input variables (six out of seven). In this case, collinearity was more likely to occur, and, therefore, the estimation ability was lower. Although GDD led to a simple changing trend over time, it concealed the impacts of other factors, and the MLR models failed to capture the resulting variability. These may lead to non-linear relationships between each N status indicator and the combination of these sensing indices and GDD, which is not suitable to be simulated by MLR functions.

As an attractive and powerful machine learning method, RFR model has strong capabilities in processing large numbers of input variables and exploring complex relationships between spectral signatures and crop N status indicators using non-linear regression algorithms. Thus, it is easy to understand the optimal accuracy in maize N status estimation achieved by the RFR models (Table 7, Table 9 and Figure 4). Furthermore, the higher importance of GDD among all the variables in the RFR models further verified the potential of introducing GDD to characterize crop N status under various environmental conditions at different times, as stated in previous studies [32,68,69]. Nevertheless, compared with SR models based on the modified fluorescence indices, the improvements of R^2, RMSE, and RE in the validation results using the RFR modeling were not very remarkable (Figure 4). However, obvious better distributions of the points that were closer to the 1:1 line were found in the scatter plots based on the validation results of all three N indicators using the RFR method (Figure 4), and the density curves of the observed N status values estimated by RFR models were most similar to those of the observed N status values, although with some discrepancies (Figure 5). However, it should be noted that a relatively small dataset was used for model testing (n = 126) and training (n = 252). The RFR algorithm has been proven to be efficient in processing massive data [39,70]. Therefore, higher RFR model validation accuracy and Kappa value might be achieved when using a larger dataset. Furthermore, NNI seemed to be most difficult to be estimated well with the lowest accuracy. This was true for all three modeling approaches (Figure 4). Although ranked second in NNI estimation, the importance of GDD was not remarkably different from other sensing variables (Table 7). More input variables may need to be included to improve the prediction of NNI as well as other N status indicators.

5. Conclusions

This study examined and verified that the fluorescence sensor Multiplex is a promising tool for N variability detection and N nutritional status estimation in maize. The Multiplex indices (ratios of signals from separate detectors) were more suitable to distinguish plants under different N treatments than the data from the individual detectors. Moreover, the optimal N status monitoring capacity was achieved as early as the V6 growth stage. Normalizing the fluorescence indices by GDD was an efficient method to reduce the influence of different years and growth stages. The MLR models did not estimate PNC, PNU, and NNI well across years and growth stages through data fusion of Multiplex indices and GDD, while the SR models based on modified fluorescence indices provided acceptable validation results. In contrast, the non-linear RFR approach showed the most

reliable and robust performance and achieved the best estimation power. More research is needed to further improve the RFR models using a larger set of input variables as well as more sampling points for maize N status estimation across diverse conditions using fluorescence sensing technologies.

Author Contributions: Conceptualization and methodology, R.D., Y.M. and X.W.; validation, Y.M.; formal analysis, R.D.; investigation, R.D. and X.W.; data curation, R.D.; writing—original draft preparation, R.D.; writing—review and editing, Y.M., F.Y. and K.K.; project administration, Y.M., K.K. All authors have read and agreed to the published version of the manuscript.

Funding: This research was funded by Norwegian Ministry of Foreign Affairs (SINOGRAIN II, CHN-17/0019), Key National Research and Development Program (2016YFD0200600; 2016YFD0200602), the UK Biotechnology and Biological Sciences Research Council (BB/P004555/1), and USDA National Institute of Food and Agriculture (State project 1016571).

Institutional Review Board Statement: Not applicable.

Informed Consent Statement: Informed consent was obtained from all subjects involved in the study.

Data Availability Statement: The data presented in this study are available on request from the corresponding author. The data are not yet publicly available.

Acknowledgments: We would like to thank Zhichao Chen, Xuezhi Yue, Zheng Fang, Weidong Lou, Guiyin Jiang and Yue Li for their assistance in field experiments and data collection.

Conflicts of Interest: The authors declare no conflict of interest.

References

1. Kant, S.; Bi, Y.; Rothstein, S.J. Understanding plant response to nitrogen limitation for the improvement of crop nitrogen use efficiency. *J. Exp. Bot.* **2011**, *62*, 1499–1509. [CrossRef] [PubMed]
2. Reddy, M.M.; Ulaganathan, K. Nitrogen nutrition, its regulation and biotechnological approaches to improve crop productivity. *Am. J. Plant Sci.* **2015**, *6*, 2745–2798. [CrossRef]
3. Jaynes, D.B.; Colvin, T.S.; Karlen, D.L.; Cambardella, C.A.; Meek, D.W. Nitrate loss in subsurface drainage as affected by nitrogen fertilizer rate. *J. Environ. Qual.* **2001**, *30*, 1305–1314. [CrossRef] [PubMed]
4. Sinclair, R.T.; Rufty, T.W. Nitrogen and water resources commonly limit crop yield increases, not necessarily plant genetics. *Glob. Food Sec.* **2012**, *1*, 94–98. [CrossRef]
5. Lassaletta, L.; Billen, G.; Garnier, J.; Bouwman, L.; Velazquez, E.; Mueller, N.D.; Gerber, J.S. Nitrogen use in the global food system: Past trends and future trajectories of agronomic performance, pollution, trade, and dietary demand. *Environ. Res. Lett.* **2016**, *11*, 095007. [CrossRef]
6. Ali, M.M.; Al-Ani, A.; Eamus, D.; Tan, D.K.Y. Leaf nitrogen determination using non-destructive techniques—A review. *J. Plant Nutr.* **2017**, *40*, 928–953. [CrossRef]
7. Colaço, A.F.; Bramley, R.G.V. Do crop sensors promote improved nitrogen management in grain crops? *Field Crops Res.* **2018**, *218*, 126–140. [CrossRef]
8. Berger, K.; Verrelst, J.; Féret, J.-B.; Wang, Z.; Wocher, M.; Strathmann, M.; Danner, M.; Mauser, W.; Hank, T. Crop nitrogen monitoring: Recent progress and principal developments in the context of imaging spectroscopy missions. *Remote Sens. Environ.* **2020**, *242*, 111758. [CrossRef]
9. Karthikeyan, L.; Chawla, I.; Mishra, A.K. A review of remote sensing applications in agriculture for food security: Crop growth and yield, irrigation, and crop losses. *J. Hydrol.* **2020**, *586*, 124905. [CrossRef]
10. Cao, Q.; Miao, Y.; Wang, H.; Huang, S.; Cheng, S.; Khosla, R.; Jiang, R. Non-destructive estimation of rice plant nitrogen status with Crop Circle multispectral active canopy sensor. *Field Crops Res.* **2013**, *154*, 133–144. [CrossRef]
11. Cao, Q.; Miao, Y.; Feng, G.; Gao, X.; Li, F.; Liu, B.; Yue, S.; Cheng, S.; Ustin, S.L.; Khosla, R. Active canopy sensing of winter wheat nitrogen status: An evaluation of two sensor systems. *Comput. Electron. Agric.* **2015**, *112*, 54–67. [CrossRef]
12. Huang, S.; Miao, Y.; Zhao, G.; Yuan, F.; Ma, X.; Tan, C.; Yu, W.; Gnyp, M.L.; Lenz-Wiedemann, V.I.S.; Rascher, U.; et al. Satellite remote sensing-based in-season diagnosis of rice nitrogen status in Northeast China. *Remote Sens.* **2015**, *7*, 10646–10667. [CrossRef]
13. Li, F.; Miao, Y.; Feng, G.; Yuan, F.; Yue, S.; Gao, X.; Liu, Y.; Liu, B.; Ustin, S.L.; Chen, X. Improving estimation of summer maize nitrogen status with red edge-based spectral vegetation indices. *Field Crops Res.* **2014**, *157*, 111–123. [CrossRef]
14. Heege, H.J.; Reusch, S.; Thiessen, E. Prospects and results for optical systems for site-specific on-the-go control of nitrogen-top-dressing in Germany. *Precis. Agric.* **2008**, *9*, 115–131. [CrossRef]
15. Fu, Y.; Yang, G.; Pu, R.; Li, Z.; Li, H.; Xu, X.; Song, X.; Yang, X.; Zhao, C. An overview of crop nitrogen status assessment using hyperspectral remote sensing: Current status and perspectives. *Eur. J. Agron.* **2021**, *124*, 126241. [CrossRef]

16. Tremblay, N.; Wang, Z.; Cerovic, Z.G. Sensing crop nitrogen status with fluorescence indicators. A review. *Agron. Sustain. Dev.* **2012**, *32*, 451–464. [CrossRef]
17. Longchamps, L.; Khosla, R. Early detection of nitrogen variability in maize using fluorescence. *Agron. J.* **2014**, *106*, 511–518. [CrossRef]
18. Huang, S.; Miao, Y.; Yuan, F.; Cao, Q.; Ye, H.; Lenz-Wiedemann, V.I.S.; Bareth, G. In-Season diagnosis of rice nitrogen status using proximal fluorescence canopy sensor at different growth stages. *Remote Sens.* **2019**, *11*, 1847. [CrossRef]
19. Zarco-Tejada, P.J.; Miller, J.R.; Mohammed, G.H.; Noland, T.L.; Sampson, P.H. Vegetation stress detection through chlorophyll a+b estimation and fluorescence effects on hyperspectral imagery. *J. Environ. Qual.* **2002**, *31*, 1433–1441. [CrossRef] [PubMed]
20. Campbell, P.K.; Middleton, E.M.; McMurtrey, J.E.; Corp, L.A.; Chappelle, E.W. Assessment of vegetation stress using reflectance or fluorescence measurements. *J. Environ. Qual.* **2007**, *36*, 832–845. [CrossRef] [PubMed]
21. Zhang, Y.; Tremblay, N.; Zhu, J. A first comparison of Multiplex® for the assessment of corn nitrogen status. *J. Food Agric. Environ.* **2012**, *10*, 1008–1016.
22. Agati, G.; Foschi, L.; Grossi, N.; Guglielminetti, L.; Cerovic, Z.G.; Volterrani, M. Fluorescence-based versus reflectance proximal sensing of nitrogen content in *Paspalum vaginatum* and *Zoysia matrella* turfgrasses. *Eur. J. Agron.* **2013**, *45*, 39–51. [CrossRef]
23. Li, J.W.; Zhang, J.X.; Zhao, Z.; Lei, X.D.; Xu, X.L.; Lu, X.X.; Weng, D.L.; Gao, Y.; Cao, L.K. Use of fluorescence-based sensors to determine the nitrogen status of paddy rice. *J. Agric. Sci.* **2013**, *151*, 862–871. [CrossRef]
24. Padilla, F.M.; Gallardo, M.; Peña-Fleitas, M.T.; de Souza, R.; Thompson, R.B. Proximal optical sensors for nitrogen management of vegetable crops: A review. *Sensors* **2018**, *18*, 2083. [CrossRef]
25. Padilla, F.M.; Peña-Fleitas, M.T.; Gallardo, M.; Thompson, R.B. Proximal optical sensing of cucumber crop N status using chlorophyll fluorescence indices. *Eur. J. Agron.* **2016**, *73*, 83–97. [CrossRef]
26. Cilia, C.; Panigada, C.; Rossini, M.; Meroni, M.; Busetto, L.; Amaducci, S.; Boschetti, M.; Picchi, V.; Colombo, R. Nitrogen status assessment for variable rate fertilization in maize through hyperspectral imagery. *Remote Sens.* **2014**, *6*, 6549–6565. [CrossRef]
27. Wang, Y.; Ye, Y.; Huang, Y.; Zhao, Y.; Ren, N.; Fu, W.; Yue, S. Development of nitrogen fertilizer topdressing model for winter wheat based on critical nitrogen dilution curve. *Int. J. Plant Prod.* **2020**, *14*, 165–175. [CrossRef]
28. Wang, Y.; Shi, P.; Ji, R.; Min, J.; Shi, W.; Wang, D. Development of a model using the nitrogen nutrition index to estimate in-season rice nitrogen requirement. *Field Crops Res.* **2020**, *245*, 107664. [CrossRef]
29. Bronson, K.F. Optimal internal nitrogen use efficiency for irrigated cotton in the southwestern United States. *Agron. J.* **2021**, *113*, 2821–2831. [CrossRef]
30. Lu, J.; Miao, Y.; Shi, W.; Li, J.; Yuan, F. Evaluating different approaches to nondestructive nitrogen status diagnosis of rice using portable RapidSCAN active canopy sensor. *Sci. Rep.* **2017**, *7*, 14073. [CrossRef]
31. Dong, R.; Miao, Y.; Wang, X.; Chen, Z.; Yuan, F. Improving maize nitrogen nutrition index prediction using leaf fluorescence sensor combined with environmental and management variables. *Field Crops Res.* **2021**, *269*, 108180. [CrossRef]
32. Samborski, S.M.; Tremblay, N.; Fallon, E. Strategies to make use of plant sensors-based diagnostic information for nitrogen recommendations. *Agron. J.* **2009**, *101*, 800–816. [CrossRef]
33. Muñoz-Huerta, R.F.; Guevara-Gonzalez, R.G.; Contreras-Medina, L.M.; Torres-Pacheco, I.; Prado-Olivarez, J.; Ocampo-Velazquez, R.V. A review of methods for sensing the nitrogen status in plants: Advantages, disadvantages and recent advances. *Sensors* **2013**, *13*, 10823–10843. [CrossRef]
34. Padilla, F.M.; Farneselli, M.; Gianquinto, G.; Tei, F.; Thompson, R.B. Monitoring nitrogen status of vegetable crops and soils for optimal nitrogen management. *Agric. Water Manag.* **2020**, *241*, 106356. [CrossRef]
35. Dong, R.; Miao, Y.; Wang, X.; Chen, Z.; Yuan, F.; Zhang, W.; Li, H. Estimating plant nitrogen concentration of maize using a leaf fluorescence sensor across growth stages. *Remote Sens.* **2020**, *12*, 1139. [CrossRef]
36. Yao, X.; Huang, Y.; Shang, G.; Zhou, C.; Cheng, T.; Tian, Y.; Cao, W.; Zhu, Y. Evaluation of six algorithms to monitor wheat leaf nitrogen concentration. *Remote Sens.* **2015**, *7*, 14939. [CrossRef]
37. Pullanagari, R.R.; Kereszturi, G.; Yule, I.J. Mapping of macro and micro nutrients of mixed pastures using airborne AisaFENIX hyperspectral imagery. *Isprs J. Photogramm.* **2016**, *117*, 1–10. [CrossRef]
38. Zhou, K.; Cheng, T.; Zhu, Y.; Cao, W.X.; Ustin, S.L.; Zheng, H.B.; Yao, X.; Tian, Y.C. Assessing the impact of spatial resolution on the estimation of leaf nitrogen concentration over the full season of paddy rice using near-surface imaging spectroscopy data. *Front. Plant Sci.* **2018**, *9*, 964. [CrossRef]
39. Verrelst, J.; Camps-Valls, G.; Muñoz-Marí, J.; Rivera, J.P.; Veroustraete, F.; Clevers, J.G.P.W.; Moreno, J. Optical remote sensing and the retrieval of terrestrial vegetation bio-geophysical properties—A review. *ISPRS J. Photogramm.* **2015**, *108*, 273–290. [CrossRef]
40. Zha, H.; Miao, Y.; Wang, T.; Li, Y.; Zhang, J.; Sun, W.; Feng, Z.; Kusnierek, K. Improving unmanned aerial vehicle remote sensing-based rice nitrogen nutrition index prediction with machine learning. *Remote Sens.* **2020**, *12*, 215. [CrossRef]
41. Wang, X.; Miao, Y.; Dong, R.; Zha, H.; Xia, T.; Chen, Z.; Kusnierek, K.; Mi, G.; Sun, H.; Li, M. Machine learning-based in-season nitrogen status diagnosis and side-dress nitrogen recommendation for corn. *Eur. J. Agron.* **2021**, *123*, 126193. [CrossRef]
42. Abendroth, L.J.; Elmore, R.W.; Boyer, M.J.; Marley, S.K. *Corn Growth and Development (Extension Publication PM 1009)*; Iowa State University Extension: Ames, IA, USA, 2011.
43. Nelson, D.W.; Sommers, L.E. Determination of total nitrogen in plant material. *Agron. J.* **1973**, *65*, 109–112. [CrossRef]
44. Li, W.; He, P.; Jin, J. Critical nitrogen curve and nitrogen nutrition index for spring maize in North-east China. *J. Plant Nutr.* **2012**, *35*, 1747–1761. [CrossRef]

45. Abraham, A.; Pedregosa, F.; Eickenberg, M.; Gervais, P.; Mueller, A.; Kossaifi, J.; Gramfort, A.; Thirion, B.; Varoquaux, G. Machine learning for neuroimaging with scikit-learn. *Front. Neuroinform.* **2014**, *8*, 14. [CrossRef]
46. Silverman, B.W. *Density Estimation for Statistics and Data Analysis*, 1st ed.; Chapman and Hall/CRC: London, UK, 1986.
47. Xia, T.; Miao, Y.; Wu, D.; Shao, H.; Khosla, R.; Mi, G. Active optical sensing of spring corn for in-season diagnosis of nitrogen status based on nitrogen nutrition index. *Remote Sens.* **2016**, *8*, 605. [CrossRef]
48. Viera, A.J.; Garrett, J.M. Understanding interobserver agreement: The kappa statistic. *Fam. Med.* **2005**, *37*, 360–363.
49. Bausch, W.C.; Khosla, R. QuickBird satellite versus ground-based multi-spectral data for estimating nitrogen status of irrigated maize. *Precis. Agric.* **2010**, *11*, 274–290. [CrossRef]
50. Agati, G.; Foschi, L.; Grossi, N.; Volterrani, M. In field non-invasive sensing of the nitrogen status in hybrid bermudagrass (*Cynodon dactylon* × *C. transvaalensis* Burtt Davy) by a fluorescence-based method. *Europ. J. Agron.* **2015**, *63*, 89–96. [CrossRef]
51. Wang, X.; Miao, Y.; Batchelor, W.D.; Dong, R.; Kusnierek, K. Evaluating model-based strategies for in-season nitrogen management of maize using weather data fusion. *Agric. For. Meteorol.* **2021**, *308–309*, 108564. [CrossRef]
52. Bragazza, L.; Freeman, C. High nitrogen availability reduces polyphenol content in *Sphagnum* peat. *Sci. Total Environ.* **2007**, *377*, 439–443. [CrossRef] [PubMed]
53. Liu, W.; Zhu, D.; Liu, D.; Geng, M.; Zhou, W.; Mi, W. Influence of nitrogen on the primary and secondary metabolism and synthesis of flavonoids in *Chrysanthemum morifolium* Ramat. *J. Plant Nutr.* **2010**, *33*, 240–254. [CrossRef]
54. Hichem, H.; Mounir, D.; Naceur, E.A. Differential responses of two maize (*Zea mays* L.) varieties to salt stress: Changes on polyphenols composition of foliage and oxidative damages. *Ind. Crop. Prod.* **2009**, *30*, 144–151. [CrossRef]
55. Agati, G.; Cerovic, Z.G.; Pinelli, P.; Tattini, M. Light-induced accumulation of ortho-dihydroxylated flavonoids as non-destructively monitored by chlorophyll fluorescence excitation techniques. *Environ. Exp. Bot.* **2011**, *73*, 3–9. [CrossRef]
56. Agati, G.; Brunetti, C.; Di Ferdinando, M.; Ferrini, F.; Pollastri, S.; Tattini, M. Functional roles of flavonoids in photoprotection: New evidence, lessons from the past. *Plant Physiol. Biochem.* **2013**, *72*, 35–45. [CrossRef]
57. Edwards, J. *Maize Growth & Development*; NSW Department of Primary Industries: Orange, NSW, Australia, 2009.
58. Hank, T.B.; Berger, K.; Bach, H.; Clevers, J.G.P.W.; Gitelson, A.; Zarco-Tejada, P.; Mauser, W. Spaceborne imaging spectroscopy for sustainable agriculture: Contributions and challenges. *Surv. Geophys.* **2019**, *40*, 515–551. [CrossRef]
59. Pinter, P.J.; Hatfield, J.L.; Schepers, J.S.; Barnes, E.M.; Moran, M.S.; Daughtry, C.S.T.; Upchurch, D.R. Remote sensing for crop management. *Photogramm. Eng. Remote. Sens.* **2003**, *69*, 647–664. [CrossRef]
60. Andersen, R.A.; Kasperbauer, M.J. Effects of near-ultraviolet radiation and temperature on soluble phenols in *Nicotiana tabacum*. *Phytochemistry* **1971**, *10*, 1229–1232. [CrossRef]
61. Barnes, P.W.; Searles, P.S.; Ballaré, C.L.; Ryel, R.J.; Caldwell, M.M. Noninvasive measurements of leaf epidermal transmittance of UV radiation using chlorophyll fluorescence: Field and laboratory studies. *Physiol. Plant* **2000**, *109*, 274–283. [CrossRef]
62. Fu, Y.; Yang, G.; Li, Z.; Li, H.; Li, Z.; Xu, X.; Song, X.; Zhang, Y.; Duan, D.; Zhao, C.; et al. Progress of hyperspectral data processing and modelling for cereal crop nitrogen monitoring. *Comput. Electron. Agric.* **2020**, *172*, 105321. [CrossRef]
63. Zhang, J.; Qiu, X.; Wu, Y.; Zhu, Y.; Cao, Q.; Liu, X.; Cao, W. Combining texture, color, and vegetation indices from fixed-wing UAS imagery to estimate wheat growth parameters using multivariate regression methods. *Comput. Electron. Agric.* **2021**, *185*, 106138. [CrossRef]
64. Palka, M.; Manschadi, A.M.; Koppensteiner, L.; Neubauer, T.; Fitzgerald, G.J. Evaluating the performance of the CCCI-CNI index for estimating N status of winter wheat. *Europ. J. Agron.* **2021**, *130*, 126346. [CrossRef]
65. Ji, R.; Shi, W.; Wang, Y.; Zhang, H.; Min, J. Nondestructive estimation of bok choy nitrogen status with an active canopy sensor in comparison to a chlorophyll meter. *Pedosphere* **2020**, *30*, 769–777. [CrossRef]
66. Debaeke, P.; Rouet, P.; Justes, E. Relationship between the normalized SPAD index and the nitrogen nutrition index: Application to durum wheat. *J. Plant Nutr.* **2006**, *29*, 75–92. [CrossRef]
67. Ziadi, N.; Brassard, M.; Bélanger, G.; Claessens, A.; Tremblay, N.; Cambouris, A.N.; Nolin, M.C.; Parent, L.E. Chlorophyll measurements and nitrogen nutrition index for the evaluation of corn nitrogen status. *Agron. J.* **2008**, *100*, 1264–1273. [CrossRef]
68. Teal, R.K.; Tubana, B.; Girma, K.; Freeman, K.W.; Arnall, D.B.; Walsh, O.; Raun, W.R. In-season prediction of corn grain yield potential using normalized difference vegetation index. *Agron. J.* **2006**, *98*, 1488–1494. [CrossRef]
69. Varvel, G.E.; Wilhelm, W.W.; Shanahan, J.F.; Schepers, J.S. An algorithm for corn nitrogen recommendations using a chlorophyll meter based sufficiency index. *Agron. J.* **2007**, *99*, 701–706. [CrossRef]
70. Verrelst, J.; Muñoz, J.; Alonso, L.; Delegido, J.; Rivera, J.P.; Camps-Valls, G.; Moreno, J. Machine learning regression algorithms for biophysical parameter retrieval: Opportunities for sentinel-2 and -3. *Remote Sens. Environ.* **2012**, *118*, 127–139. [CrossRef]